International Journal of Pharmaceutics 378 (2009) 37–44

Contents lists available at ScienceDirect

International Journal of Pharmaceutics

journal homepage: www.elsevier.com/locate/ijpharm

Audible acoustics in high-shear wet granulation: Application of frequency filtering

Erin M. Hansuld [a], Lauren Briens [a,*], Joe A.B. McCann [b], Amyn Sayani [b]

[a] The Western Fluidization Group, Faculty of Engineering, The University of Western Ontario, London, Ontario, N6A 5B9, Canada
[b] GlaxoSmithKline Inc., Pharmaceutical Development, Mississauga, Ontario, L5N 6L4, Canada

ARTICLE INFO

Article history:
Received 19 September 2008
Received in revised form 15 May 2009
Accepted 19 May 2009
Available online 27 May 2009

Keywords:
Acoustics
Process analytical technology
Fast Fourier transform
Partial least squares discriminant analysis
High-shear wet granulation
Granulation end-point

ABSTRACT

Previous work has shown analysis of audible acoustic emissions from high-shear wet granulation has potential as a technique for end-point detection. In this research, audible acoustic emissions (AEs) from three different formulations were studied to further develop this technique as a process analytical technology. Condenser microphones were attached to three different locations on a PMA-10 high-shear granulator (air exhaust, bowl and motor) to target different sound sources. Size, flowability and tablet break load data was collected to support formulator end-point ranges and interpretation of AE analysis. Each formulation had a unique total power spectral density (PSD) profile that was sensitive to granule formation and end-point. Analyzing total PSD in 10 Hz segments identified profiles with reduced run variability and distinct maxima and minima suitable for routine granulation monitoring and end-point control. A partial least squares discriminant analysis method was developed to automate selection of key 10 Hz frequency groups using variable importance to projection. The results support use of frequency refinement as a way forward in the development of acoustic emission analysis for granulation monitoring and end-point control.

1. Introduction

Regulatory guidance on process analytical technologies (PAT) encourages the pharmaceutical industry to develop innovative tools for monitoring product quality and improving process understanding (U.S. Department of Health and Human Services, et al., 2004). High-shear wet granulation is an integral pharmaceutical operation used to reduce segregation, enhance flowability and improve tabletting performance of powders (Aulton, 2002; Iveson et al., 2001). This is achieved through coalescence of primary particles into larger agglomerates, or granules, by spraying a liquid binder while applying shearing and compaction forces (Aulton, 2002; Parikh, 1997). The process is complex with a large number of critical variables that interact dynamically to influence final product quality, including: binder content, surface tension, viscosity, particle size, humidity, temperature and mixing speed (Iveson et al., 2001; Watano, 2007). As a result, process monitoring and control are not straightforward, and to ensure quality there is a need to develop PATs. To date, the following PATs have been investigated for granulation: power consumption/torque monitoring, near-infrared spectroscopy, imaging and vibration sensors (Faure et al., 2001; Hardy and Cook, 2003; Räsänen and Sandler, 2007); however, none of these methods have been adopted in day-to-day pharmaceutical operations.

1.1. Granulation monitoring using acoustic sensors

Recent work with ultrasonic (greater than 20,000 Hz) and audible (approximately 20–20,000 Hz) acoustic emission (AE) sensors supports their development as PAT tools for granulation monitoring and control (Whitaker et al., 2000; Briens et al., 2007; Daniher et al., 2008; Papp et al., 2008). Whitaker et al. (2000) and Papp et al. (2008) attached ultrasonic sensors to the bottom of granulator bowls to detect AEs from granules contacting the bowl wall near the sensors. Resulting acoustic profiles showed AEs were related to granule size distribution and powder flowability. Audible AEs differ significantly from ultrasonic AEs because they propagate through air with minimal attenuation (Bass et al., 2008) and therefore equipment contact is not required for detection. Briens et al. (2007) and Daniher et al. (2008) showed microphones suspended at the top of PMA-10 and PMA-25 granulator air exhausts were sensitive to granulation of a lactose based placebo formulation, while microphones on the side and bottom of the bowl were unresponsive. The mean frequency profile and root mean square sound pressure levels for one-third octave bands were found to be effective for identifying granulation end-point (Briens et al., 2007; Daniher et al., 2008).

* Corresponding author. Tel.: +1 519 661 2111 88849.
E-mail address: lbriens@eng.uwo.ca (L. Briens).

0378-5173/$ – see front matter © 2009 Elsevier B.V. All rights reserved.
doi:10.1016/j.ijpharm.2009.05.042

1.2. Multivariate analysis

Partial least squares discriminant analysis (PLS-DA) is a form of multivariate analysis introduced in this work to assess the frequency content of the AEs. Multivariate analysis has been recognized in other research for its ability to handle large, noisy and correlated data sets without ill-conditioning (Wold et al., 2001). In PLS-DA, a response matrix (Y) is used to classify each observation in a variable matrix (X) based on pre-existing knowledge. The model then seeks to simultaneously describe the structure of the X and Y matrices, while also explaining the relationship between X and Y. This is accomplished by projecting each observation into a reduced dimensional space using linear combinations of the original variables. As a result, the end model can be used to distinguish between the defined classes, such as wetting and end-point (Miletic et al., 2004; Berrueta et al., 2007). Variable importance to projection (VIP) can be used to assess the influence of each X variable in the model, where a VIP greater than one indicates above average significance (Wold et al., 2001; Chong and Jun, 2005). Work by Chong and Jun (2005) identified VIP as the preferred method for selecting relevant predictors and suggested the method is relatively insensitive to noise. VIP has mainly been applied as a bioinformatics technique to identify key variables for prediction (Hemmateenejad and Mohajeri, 2007; Musumarra et al., 2007; Mohajeri et al., 2008) or classification (Sun, 2004; Yoo and Gernaey, 2008).

1.3. Objective

The objective was to investigate the use of audible AE analysis for detecting granulation end-point with three different formulations, incorporating physical analysis to explain changes in the resulting profiles. PLS-DA was examined as a method for simplifying the identification of key frequency groups related to granulation stage, i.e. wetting, end-point or over-wet.

2. Materials and methods

2.1. Formulation

The platform granule formulation consisted of mannitol (Pearlitol® 160C, Roquette), microcrystalline cellulose (Avicel® PH 101, FMC Biopolymer), hypromellose 2910 (Pharmacoat® 603, Shin-Etsu Chemical Co.) and croscarmellose sodium (AcDiSol®, FMC Biopolymer). Two additional formulations were prepared by replacing 71% of the mannitol with maize starch (Maize Starch B, Roquette) or dextrose anhydrous (Roquette). The purpose of the substitutions was to vary the properties of the formulation by choosing starch to simulate an insoluble active and dextrose to simulate a soluble active. To achieve a 60% bowl fill, the batch sizes were 2.85 kg for mannitol and dextrose and 2.56 kg for starch. Magnesium stearate (HyQual®, Mallinckrodt Inc.) and additional croscarmellose sodium were added prior to tabletting.

2.2. Granulation method

Materials for each batch were passed through an 850 μm sieve and granulated in a Niro-Fielder PMA-10 high-shear granulator. The impeller (360 rpm) and chopper (3000 rpm) speeds were constant throughout dry mixing (5 min) and water addition (12.5–17 min). Water was added at 80 mL/min (20 psi) through a spray nozzle positioned left-of-center.

2.3. Granule analysis

2.3.1. Formulator end-point

The granulation end-point range was determined in duplicate for each formulation by stopping the granulation in 50–100 mL increments and analyzing the granules to determine if end-point had been reached.

2.3.2. Particle size

Granulations were stopped at different extents of binder addition and samples (approximately 20 g) were withdrawn opposite the nozzle and chopper. Samples were tray dried to less than 2% loss on drying (LOD) using a GCA convection oven (80 °C). LOD was determined using a Mettler Toledo Moisture Analyzer and approximately 2 g of sample. Particle size distribution was measured using an ATM Sonic Sifter with a pulse amplitude of 9 and a 5 min sift/pulse setting. The sieve set consisted of 150, 180, 250, 355, 600 and 850 μm sieves and a fines collector.

2.3.3. Flowability

Granulations were stopped at different extents of binder addition and discharged from the granulator. The material was divided in half by weight and one half was dried using a Glatt GPCG-3 fluid-bed dryer (60 °C). Mannitol and starch granules were dried to less than 2% LOD and dextrose granules were dried to less than 3% LOD. The dried granules were passed through a screen with round, 190 μm perforations using a Quadro 197 comil (1500 rpm). A 50 g sample of comilled granules was withdrawn for flowability analysis. Flowability was measured by avalanche method using a Mercury Scientific Revolution Powder Analyzer. The comilled granules (83 mL) were placed in a disk (25% fill) and rotated at 0.3 rpm. After 30 s of preparation time, images of the avalanching powder were taken at 10 frames per second until a total of 128 avalanches occurred. The change in power (potential energy) for each avalanche and the avalanche time were determined from the digital images and used to assess granule flowability.

2.3.4. Tablet compression for break load testing

Co-milled material was blended with croscarmellose sodium and magnesium stearate in a 10 L bin using a Pharmatech blender. Materials were added separately by first sieving through a 600 μm sieve and then blending for 18 and 3 min, respectively. A Korsh XL100 tablet press, fitted with a B-turret and four alternating oval punches (8.73 by 17.49 mm) was used. The press was operated at 40 rpm and a compression force of 28 kN. For each compression force, a number of tablets were compressed to establish proper operating conditions and then 50 tablets were collected for analysis. Break load was measured across the face of 10 randomly selected tablets using a Holland C50 hardness tester.

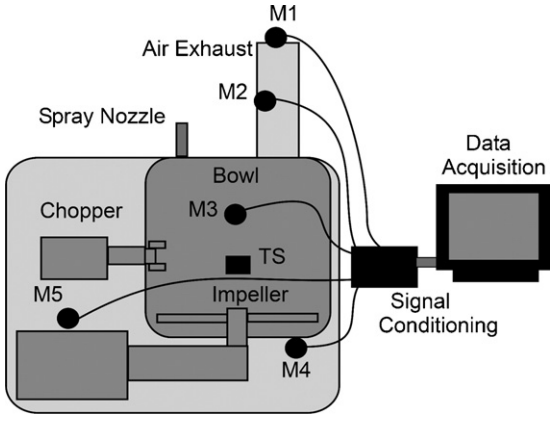

Fig. 1. Equipment setup and microphone locations (M1–M5) for PMA-10 granulator.

Table 1
End-point range summary.

Technique	Mannitol		Starch		Dextrose	
	Lower limit (mL)	Upper limit (mL)	Lower limit (mL)	Upper limit (mL)	Lower limit (mL)	Upper limit (mL)
Formulator	800	900	950	1150	900	1000
Size Distribution	800	950	1050	1250	900	1025
Flowability	800	–	950	1250	900	–
Tablet hardness	–	1000	1050	1150	–	950
End-point range	800	900	950	1150	900	1000

Abbreviations: (–) no value.

2.4. Microphone setup and data acquisition

Audible AEs were collected from five different locations on the granulator, as shown in Fig. 1. AE data was acquired at 40,000 Hz using PCB Piezotronics condenser microphones (model 130D20) and conditioned using ICP sensor signal conditioners (PCB Piezotronics). The data was logged using a National Instruments data acquisition system and LabVIEW software. 40,000 Hz was

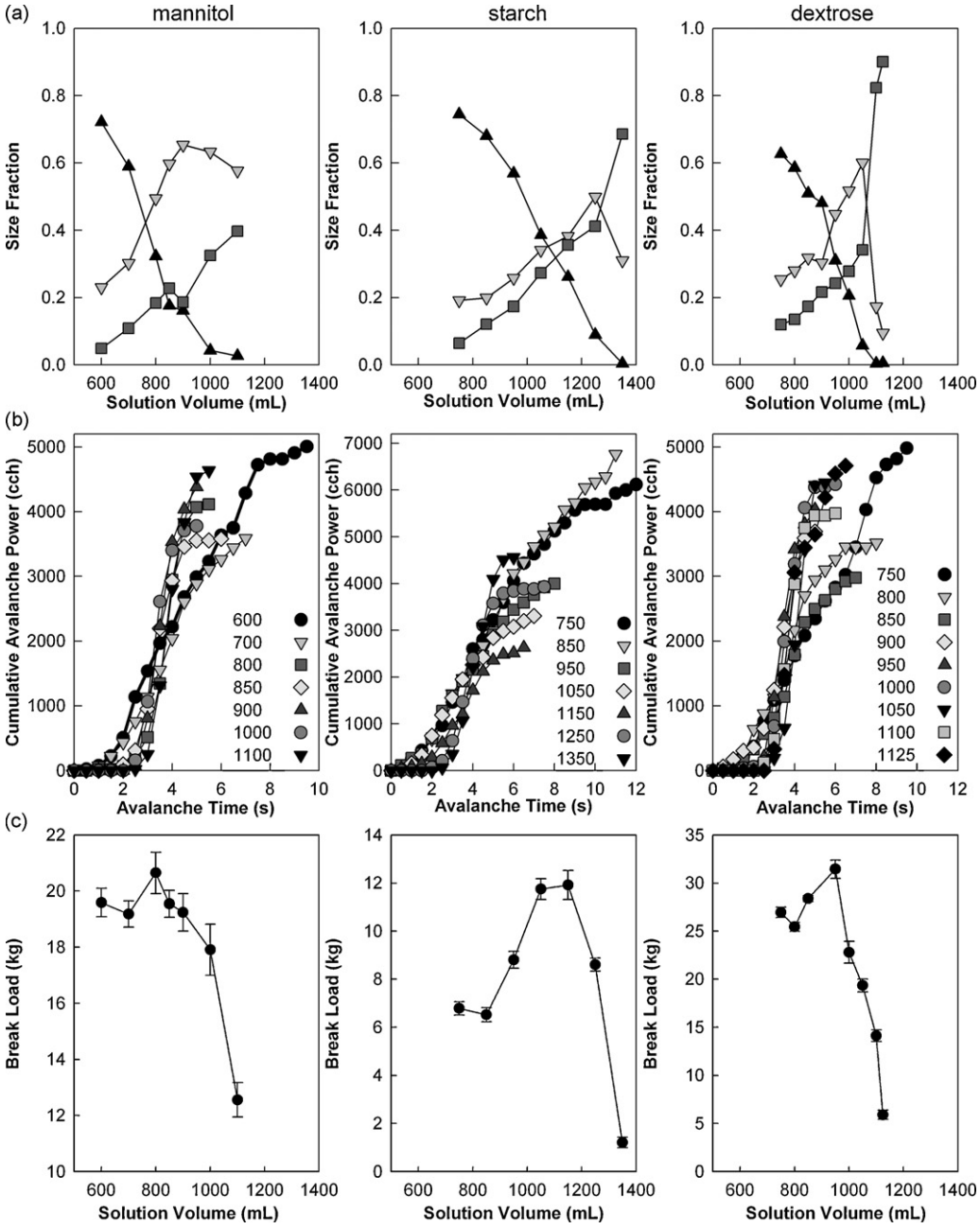

Fig. 2. (a) Size fraction versus solution volume for (▲) fines; (▼) midsize; and (■) oversize fractions. (b) Cumulative total avalanche power versus avalanche time. (c) Break load versus solution volume at 28 kN compression force. Formulations: mannitol, starch and dextrose (left to right).

selected to permit full reconstruction of the audible frequency range (20–20,000 Hz) without aliasing (Nyquist sampling theorem) (Dodson, 1992).

2.5. Signal processing

2.5.1. Fast Fourier transform

All data transformations and calculations were performed using Matlab 6.5. Power spectral density (PSD) was computed by applying fast Fourier transform analysis to 10 s consecutive data segments using the PSD function. Total PSD was determined by summing the PSDs for each time segment over the desired frequency range between 20 and 20,000 Hz. Trend lines were generated in SigmaPlot by aggregating data from five (starch) or six (mannitol and dextrose) runs and applying Loess smoothing. All results shown are for the microphone inside the air exhaust (Fig. 1).

2.5.2. Multivariate analysis

PLS-DA was used to analyze the frequency content of the acoustic signals using Umetrics' SIMCA-P+ 11.5 software. The *X* matrix was comprised of total PSDs for 10 Hz increments from 20–20,000 Hz computed over 10 s time segments and the *Y* matrix was formed using binary notation to classify each observation as wetting, end-point or over-wet. Classification was based on the formulator end-point range and supporting size, flowability and tablet analyses. The VIP analysis function in SIMCA-P was used to determine which frequency groups were most significant for describing the stages of granulation.

3. Results

3.1. Definition of end-point range

Table 1 summarizes the end-point range defined for each formulation based on formulator, size, flowability and compression analyses.

3.1.1. Size distribution

Granule size distributions were divided into fines (less than 180 μm), midsize (180–600 μm), and oversize (greater than 600 μm) fractions. Each group was plotted versus binder addition and is shown in Fig. 2a. Lower and upper end-point limits were defined by binder volumes corresponding to between 40% and 10% fines, respectively.

3.1.2. Flowability

Change in flow behaviour with binder content was determined using the avalanche method (Fig. 2b). When comparing powders, changes in avalanche power and time define a change in flow properties. For each formulation, Fig. 2b shows a distinct change in flow properties consistent with the beginning of the formulator defined end-point range (Table 1). For starch, an additional change was observed with over-wetting, between 1250 and 1350 mL, where binder addition exceeded the upper formulator end-point limit.

3.1.3. Tablet break load testing

Tablets were compressed at 28 kN from granules manufactured with different binder volumes. The resulting break loads are plotted in Fig. 2c. For mannitol, binder volumes up to 950 mL yielded tablets with similar break loads. After 1000 mL, break load decreased significantly indicating weaker tablets and defining 1000 mL as the upper end-point limit. For starch, break load reached a maximum between 1050 and 1150 mL, consistent with the formulator defined end-point range. For dextrose, break load reached a maximum at 950 mL and decreased rapidly at higher binder volumes supporting an upper end-point limit of 1000 mL.

3.2. Acoustic results

3.2.1. Microphone location

Microphones were attached to the granulator at five different locations (Fig. 1) to investigate different sources of sound. The bowl wall targeted particle-equipment contact, similar to previous ultrasonic work (Whitaker et al., 2000; Papp et al., 2008); the motor location was based on research showing impeller power consumption and torque are sensitive to granulation (Faure et al., 2001); and the air exhaust targeted AEs from the mixing and wetting process, in continuation of audible acoustic work by Briens et al. (2007) and Daniher et al. (2008). AEs collected with the microphones on the bowl and motor did not change significantly during granulation (data not shown). Both air exhaust microphones showed sensitivity to granulation, with profiles for the inside microphone (Fig. 1 M2) showing higher magnitudes due to closer proximity to granulation AEs and decreased interference from external AEs (data not shown).

Table 2
Frequency ranges identified manually and using the PLS-DA method.

Mannitol		Starch		Dextrose	
Manual (Hz)	PLS-DA (Hz)	Manual (Hz)	PLS-DA (Hz)	Manual (Hz)	PLS-DA (Hz)
100–110*	100–110[a,*]	–	30–40[b]	–	60–70[b]
110–120	110–120[a]	80–90	80–90[a]	80–90*	80–90[a,*]
–	130–140[b]	100–110*	100–110[a,*]	100–110*	100–110[a,*]
–	150–160[b]	110–120*	110–120[a,*]	110–120	110–120[a]
200–210*	200–210[a,*]	–	130–140[b]	130–140	130–140[a]
–	210–220[b]	–	150–160[b]	210–220	210–220[a]
–	270–280[b]	–	160–170[b]	–	230–240[b]
–	370–380[c]	200–210	200–210[a]	–	250–260[b]
–	450–460[c]	210–220	210–220[a]	–	260–270[b]
		–	250–260[b]	–	270–280[b]
		–	270–280[b]	–	290–300[c]
		–	1370–1380[c]	–	300–310[c]
				–	310–320[c]
				–	2970–2980[c]

Abbreviation: (–) no value.
[a] Clear profile.
[b] Noisy trend.
[c] Random noise.
* Total PSD profile shown in Fig. 4.

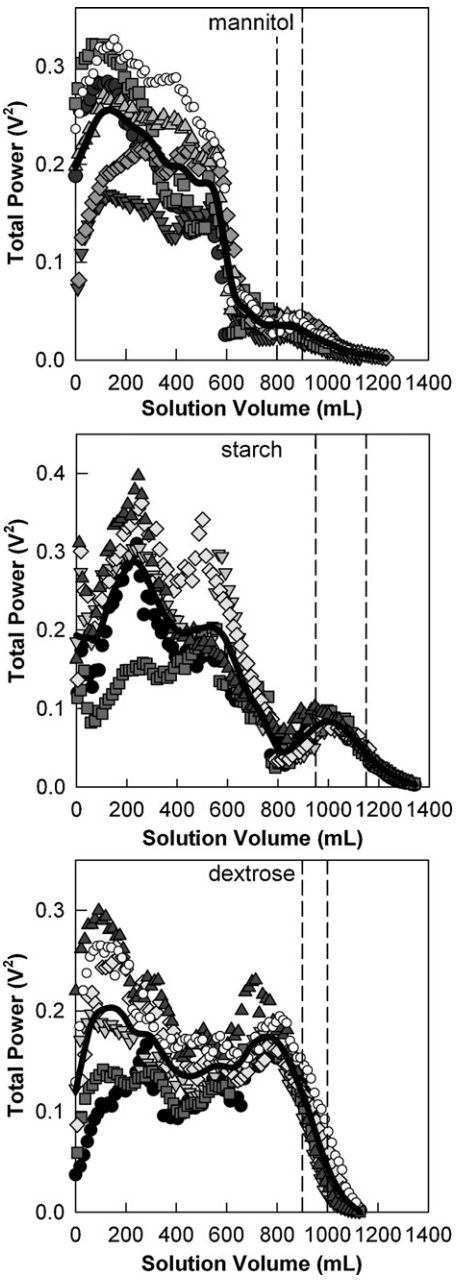

Fig. 3. Total power versus solution volume from 20–20,000 Hz. Runs defined as (●) Run 1; (▼)Run 2; (■) Run 3; (♦) Run 4; (▲) Run 5; (○) Run 6 (mannitol and dextrose only). End-point range defined by dashed vertical lines (- - -).

3.2.2. Total PSD profiles (20–20,000 Hz)

The 20–20,000 Hz total PSD profiles were unique for each formulation and all demonstrated sensitivity to granulation (Fig. 3). In each case, variability between runs was observed at the start of wetting, likely due to different particle arrangements after dry mixing. Following approximately 600 mL of binder addition, run variability was reduced and total PSD decreased gradually through each formulation's respective end-point region.

3.2.3. Frequency filtering of the 20–20,000 Hz total PSD profiles

The full frequency total PSD profiles were divided into 50 Hz groups and information relevant to granulation was observed to be concentrated below 250 Hz. The 20–250 Hz region was then divided into 10 Hz groups and each total PSD profile was manually examined for (1) reproducibility between runs and (2) distinct maxima and minima; Table 2 summarizes the 10 Hz groups that satisfied these criteria and total PSD profiles for select ranges are shown in Fig. 4.

3.2.4. Frequency filtering using VIP analysis of the PLS-DA models

For each formulation, total PSD data for 10 Hz frequency groups from 20–20,000 Hz was used to generate a PLS-DA model for each run and VIP analysis was performed. If a frequency group's VIP value was greater than one for all runs, it was retained in each PLS-DA model. VIP analysis was then repeated on the refined models to further reduce the total number of 10 Hz frequency groups (Fig. 5). The first iteration of VIP analysis reduced the number of relevant frequency groups by an average of $94 \pm 2\%$, across the three formulations. The second iteration provided an additional $90 \pm 2\%$ reduction, for an overall decrease of 99% for each formulation. The final frequency groups are summarized in Table 2 and samples of the types of profiles observed for each formulation are shown for dextrose in Fig. 6. The types of profiles are: clear profiles, with low variability between runs and significant detail throughout binder addition (80–90 Hz); profiles with visible trends but higher run variability (230–240 Hz); and profiles with no visible relationship to granulation (310–320 Hz). Since not all profile types are ideal for granulation monitoring and control, relevant frequency groups were identified by applying the manual selection criteria outlined in Section 3.2.3 (Table 2).

4. Discussion

Analysis of audible AEs from the three formulations builds on earlier research using a lactose based placebo formulation (Briens et al., 2007; Daniher et al., 2008). Together these works demonstrate that audible AEs collected in granulator air exhausts can be used for end-point detection with multiple formulations. The 10 Hz frequency groups identified for granulation monitoring and control were different for each formulation and VIP analysis showed proof of concept as a rapid approach for identifying significant frequency groups that will facilitate future work with new formulations.

4.1. Interpretation of acoustic results using physical property data

The physical data used to define granulation end-point provided a means to interpret the changes in the AE profiles. For mannitol and starch, the peaks in the end-point region corresponded to loss of fines and growth in midsize and oversize granules, a change in flow properties, and ideal tablet properties (Figs. 2–4). For mannitol, wetting resulted in a predominant increase in midsize granules compared to oversize (Fig. 2a); suggesting oversize granules formed by granule–granule agglomeration were weak and prone to breakage. For starch, wetting formed oversize and midsize granules at similar rates, until the material was over-wet and oversize granules became dominant (Fig. 2a). Comparing the total PSD profiles (Fig. 4) showed the peak in the end-point region was significantly smaller and less pronounced for mannitol than starch, suggesting its intensity is driven by the formation of oversize granules.

For dextrose, the final peaks occurred prior to end-point and corresponded to dominant fines, flow properties inconsistent with end-point flowability, and suboptimal tablet properties (Figs. 2–4). The reason for the disparity between dextrose and the other two formulations is unclear but could be the result of a different response to wetting. The reduction in PSD throughout the end-point region for all formulations is consistent with observations at similar frequencies for fluidized sand grains, where excess moisture is cited as inhibiting sound (Sholtz et al., 1997; Douady et al., 2006; Andreotti, 2004; Vriend et al., 2007). For dextrose, a different response to wetting could have resulted in AEs becoming damped before the peak related to growth in oversize granules was reached. Further studies

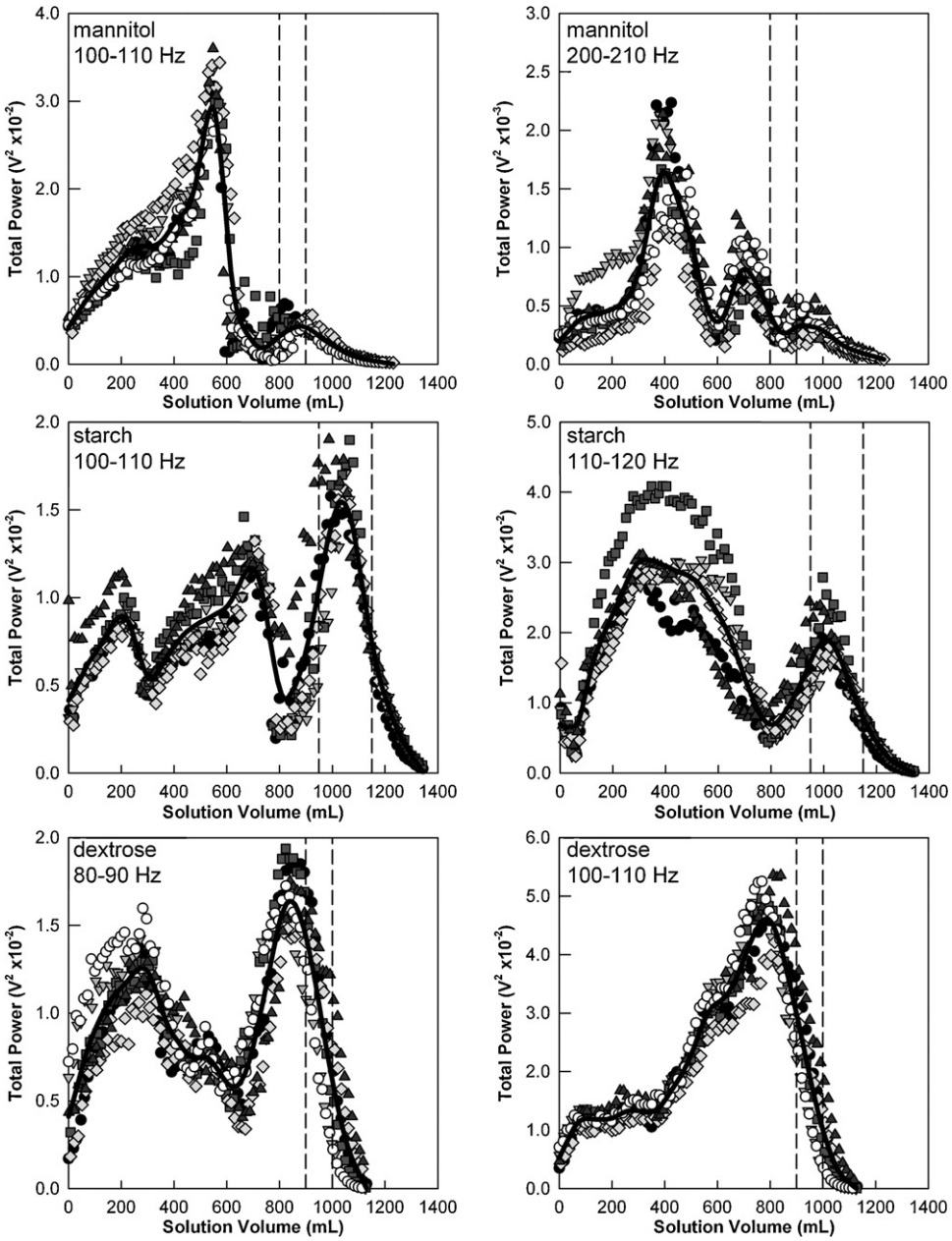

Fig. 4. Total power versus solution volume for 10 Hz frequency groups. Runs defined as (●) Run 1; (▼) Run 2; (■) Run 3; (♦) Run 4; (▲) Run 5; (○) Run 6 (mannitol and dextrose only). End-point range defined by dashed vertical lines (- - -).

are required to fully explain these observed differences in total PSD with formulation.

4.2. Important features in the 10 Hz total PSD profiles

Physical analysis defined three stages of granulation: (1) wetting, where binder was added to reach end-point; (2) end-point, where binder volumes produced optimal granules; and (3) overwet, where binder exceeded end-point requirements. Features related to both the wetting and end-point stages are critical to development of AE analysis for online use. The 20–20,000 Hz profiles (Fig. 3) would not be suitable for monitoring the wetting stage, because variability between runs was significant. Breaking the profiles into 10 Hz groups was effective for improving run reproducibility and isolating distinct maxima and minima related to granulation stage (Table 2; Fig. 4). Peaks related to end-point can be used to determine when to stop a batch and peaks during wetting can be used to monitor batch progress and anticipate end-point. More reproducible and pronounced features allow for more precise monitoring and control.

4.2.1. Mannitol

For mannitol, 10 Hz profiles showed the following early warning signals for end-point control: a local minimum 75 mL prior to end-point (100–110 Hz) and a local maximum 100 mL prior to end-point (200–210 Hz) (Fig. 4). Monitoring of the wetting stage is supported by distinct and reproducible peaks during the first 500 mL of binder addition in both 10 Hz profiles (Fig. 4).

4.2.2. Starch

For identifying end-point, the 100–110 Hz and 110–120 Hz profiles (Fig. 4) accentuated two features in the full frequency profile (Fig. 3): the local minimum approximately 150 mL before end-point and the distinct peak in the end-point region. The minimum can

be used to gauge end-point by signaling the remaining binder volume. The peak supports online end-point detection by providing a signal to stop binder addition. Both 10 Hz profiles (Fig. 4) also showed additional local maxima and minima preceding the end-point region that are suitable for assessing granulation progress.

4.2.3. Dextrose

For dextrose, end-point consistently matched a final decrease in total PSD (Figs. 3 and 4). With filtering, the peak preceding the decrease is accentuated and supports use as an early warning signal (Fig. 4). The 10 Hz profiles shown (Fig. 4) also support monitoring the wetting stage, via the gradual increase to a maximum (80–90 Hz) or the plateau followed by a gradual increase (100–110 Hz).

4.2.4. Summary

The selected 10 Hz frequency ranges (Table 2) were different for each formulation, as were the corresponding total PSD profiles (Fig. 4). Only the starch profiles showed distinct peaks within the defined end-point region; however, early warning peaks 50–100 mL prior to end-point are equally, if not more useful because they allow time for response with less risk of over-wetting. All profiles contained information during both the wetting and end-point phases; this supports ultrasonic work that suggests granulation does not produce new frequencies, but rather alters the AE intensity of existing frequencies (Papp et al., 2008).

4.3. Assessment of the PLS-DA method for identification of key frequency groups

The formulation dependency of the key frequency groups poses a challenge for further development of audible acoustics as a PAT tool, since each new formulation would require generation and analysis of nearly 2000 new graphs. The PLS-DA method (Fig. 5) was developed to simplify the review of all 10 Hz total PSD profiles (Table 2). The ability of VIP analysis to identify frequency groups satisfying the manual selection criteria outlined in Section 3.2.3. supports the use of the PLS-DA method for rapid frequency selection. VIP analysis also identified frequency groups that did not satisfy the manual selection criteria, due to the nature of the PLS-DA algorithm. For example, Fig. 6b (230–240 Hz) contains features similar to Fig. 6a (80–90 Hz) but with less defined peaks and higher run variability; therefore 230–240 Hz was likely identified because of a correlation with 80–90 Hz. Fig. 6c shows a profile with no apparent relationship to granulation stage; this frequency group was likely selected for its ability to explain differences between the frequency groups, rather than differences between granulation stages. While these extra profiles still necessitate application of manual selection criteria, the number of frequency groups to assess is considerably less and the method can be easily applied to large data sets with variable group sizes.

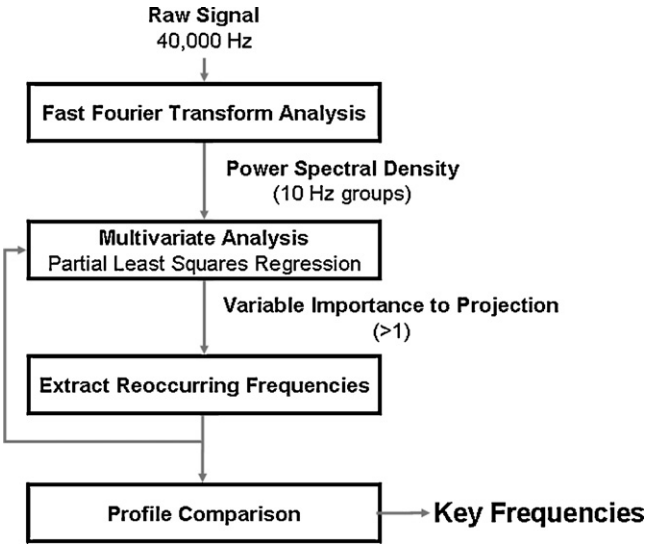

Fig. 5. PLS-DA method for selection of key frequency groups.

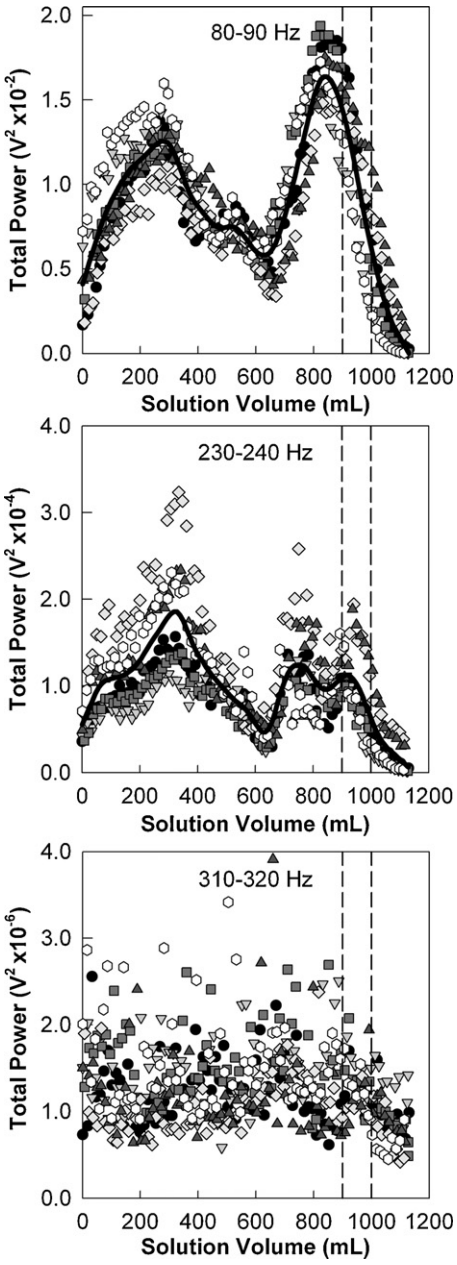

Fig. 6. Total power versus solution volume for dextrose. Runs defined as (●) Run 1; (▼) Run 2; (■) Run 3; (♦) Run 4; (▲) Run 5; (○) Run 6. End-point range defined by dashed vertical lines (- - -).

5. Conclusions

Building on proof of concept work by Briens et al. (2007) and Daniher et al. (2008), analysis of audible AEs was demonstrated to be a viable method of end-point detection for a range of formulations. The air exhaust was confirmed to be the best location for acquiring AEs related to granulation and placing the microphone

inside the air exhaust, rather than at the top, was preferred because of increased signal intensity and shelter from outside noise.

End-point ranges were defined for each formulation and supported by physical analysis to allow for objective interpretation of the acoustic results. Introduction of three additional formulations showed that although the acoustic profile is dependent on formulation, at end-point there is a consistent decrease in total PSD. Frequency filtering reduced variability between runs and 10 Hz total PSD profiles showed features suitable for online end-point detection and process monitoring. These results support the ability of audible acoustics to satisfy regulatory objectives for PAT.

PLS-DA demonstrated proof of concept as an objective method to assist with identification of key frequency groups. The work supports frequency filtering and shows potential for identifying key acoustic frequency groups in new formulations or during scale-up. In summary, audible acoustic sensors' applicability to formulations with both soluble and insoluble primary components supports further development as PAT tool.

Acknowledgments

The authors would like to thank GlaxoSmithKline Inc. and The Western Fluidization Group for their support and Zane Arp, Vijay Kumar Akunuri and Avinash Sharma (GlaxoSmithKline Inc.) for their technical contributions. The Natural Sciences and Engineering Research Council of Canada (NSERC) is also acknowledged for their financial support.

References

Andreotti, B., 2004. The song of dunes as a wave-particle mode locking. Phys. Rev. Lett. 93, 1–4.

Aulton, M. (Ed.), 2002. Pharmaceutics: The Science of Dosage Form Design, second edition. Elsevier, Spain.

Bass, H.E., Campanella, A.J., Chambers, J.P., Lindsay, R.B., 2008. Sound absorption. AccessScience@McGraw-Hill. Retrieved May 14, 2008, from http://www.accessscience.com.proxy2.lib.uwo.ca:2048, doi:10.1036/1097-8542.637300.

Berrueta, L.A., Alonso-Salces, R.M., Héberger, K., 2007. Supervised pattern recognition in food analysis. J. Chromatogr. 1158, 196–214.

Briens, L., Daniher, D., Tallevi, A., 2007. Monitoring high-shear granulation using sound and vibration measurements. Int. J. Pharm. 331, 54–60.

Chong, I., Jun, C., 2005. Performance of some variable selection methods when multicollinearity is present. Chemometr. Intell. Lab. Syst. 78, 103–112.

Daniher, D., Briens, L., Tallevi, A., 2008. End-point detection in high-shear granulation using sound and vibration signal analysis. Powder Technol. 181, 130–136.

Dodson, M., 1992. Shannon sampling theorem. Curr. Sci. 63, 253–260.

Douady, S., Manning, A., Hersen, P., Elbelrhiti, H., Protière, S., Daerr, A., Kabbachi, B., 2006. Song of the dune as a self-synchronized instrument. Phys. Rev. Lett. 97, 0180021–01800214.

Faure, A., York, P., Rowe, R.C., 2001. Process control and scale-up of pharmaceutical wet granulation processes: a review. Eur. J. Pharm. Biopharm. 52, 269–277.

Hardy, I.J., Cook, W.G., 2003. Predictive techniques for the design, optimisation and manufacture of solid dosage forms. J. Pharm. Pharmacol. 55, 3–18.

Hemmateenejad, B., Mohajeri, A., 2007. Application of quantum topological molecular similarity descriptors in QSPR study of the *o*-methylation of substituted phenols. J. Comput. Chem. 29, 266–274.

Iveson, S.M., Litster, J.D., Hapgood, K., Ennis, B.J., 2001. Nucleation, growth and breakage phenomena in agitated wet granulation processes: a review. Powder Technol. 177, 3–39.

Miletic, I., Quinn, S., Dudzic, M., Vaculik, M., Champagne, M., 2004. An industrial perspective on implementing on-line applications of multivariate statistics. J. Process Control 14, 821–836.

Mohajeri, A., Hemmateenejad, B., Mehdipour, A., Miri, R., 2008. Modeling calcium channel antagonistic activity of dihydropyridine derivatives using QTMS indices analyzed by GA-PLS and PC-GA-PLS. J. Mol. Graphics Modell. 26, 1057–1065.

Musumarra, G., Trovato-Salinaro, A., Scirè, S., Foti, A., Barresi, V., Fortuna, C.G., Strazzulla, G., Condorelli, D.F., 2007. Identification of genes involved in radiation-induced G_1 arrest. J. Chemometrics 21, 398–405.

Parikh, D.M., 1997. Handbook of pharmaceutical granulation technology drugs and pharmaceutical sciences, vol.81. Marcel Dekker Inc, New York.

Papp, M., Pujara, C., Pinal, R., 2008. Monitoring of high-shear granulation using acoustic emission: predicting granule properties. JPI 3, 113–122.

Räsänen, E., Sandler, N., 2007. Near infrared spectroscopy in the development of solid dosage forms. J. Pharm. Pharmacol. 59, 147–159.

Sholtz, P., Bretz, M., Nori, F., 1997. Sound-producing sand avalanches. Contemp. Phys. 38, 329–342.

Sun, H., 2004. Prediction of chemical carcinogenicity from molecular structure. J. Chem. Inf. Model. 44, 1506–1514.

U.S. Department of Health and Human Services, Food and Drug Administration, Center for Drug Evaluation and Research, Center for Veterinary Medicine, Office of Regulatory Affairs, 2004. Guidance for industry PAT–A framework for innovative pharmaceutical development, manufacturing, and quality assurance. Pharmaceutical CGMPs. Retrieved September 17, 2008, from www.fda.gov.cvm/guidance/published.html.

Vriend, N.M., Hunt, M.L., Clayton, R.W., Brennen, C.E., 2007. Solving the mystery of booming sand dunes. Geophys. Res. Lett. 34, L162061–L1620616.

Watano, S., 2007. In: Salman, A., Hounslow, M., Seville, J. (Eds.), Handbook of Powder Technology, vol. 11. Elsevier, The Netherlands.

Whitaker, M., Baker, G., Westrup, J., Goulding, P., Rudd, D., Belchamber, R., Collins, M., 2000. Application of acoustic emission to the monitoring and end point determination of a high shear granulation process. Int. J. Pharm. 204, 79–91.

Wold, S., Sjöström, M., Eriksson, L., 2001. PLS-regression: a basic tool of chemometrics. Chemom. Intell. Lab. Syst. 58, 109–130.

Yoo, C., Gernaey, K.V., 2008. Classification and diagnostic output prediction of cancer using gene expression profiling and supervised machine learning algorithms. J. Chem. Eng. Jpn. 41, 898–914.